Muscle-tendon length and force affect human tibialis anterior central aponeurosis stiffness in vivo

Brent James Raiteri[a,b,1], Andrew Graham Cresswell[a], and Glen Anthony Lichtwark[a]

[a]Centre for Sensorimotor Performance, School of Human Movement and Nutrition Sciences, The University of Queensland, St. Lucia, QLD 4072, Brisbane, Australia; and [b]Human Movement Science, Faculty of Sport Science, Ruhr-University Bochum, 44801 Bochum, Nordrhein-Westfalen, Germany

Edited by Silvia Salinas Blemker, University of Virginia, Charlottesville, VA, and accepted by Editorial Board Member C. O. Lovejoy February 21, 2018 (received for review July 20, 2017)

The factors that drive variable aponeurosis behaviors in active versus passive muscle may alter the longitudinal stiffness of the aponeurosis during contraction, which may change the fascicle strains for a given muscle force. However, it remains unknown whether these factors can drive variable aponeurosis behaviors across different muscle-tendon unit (MTU) lengths and influence the subsequent fascicle strains during contraction. Here, we used ultrasound and elastography techniques to examine in vivo muscle fascicle behavior and central aponeurosis deformations of human tibialis anterior (TA) during force-matched voluntary isometric dorsiflexion contractions at three MTU lengths. We found that increases in TA MTU length increased both the length and apparent longitudinal stiffness of the central aponeurosis at low and moderate muscle forces ($P < 0.01$). We also found that increased aponeurosis stiffness was directly related to reduced magnitudes of TA muscle fascicle shortening for the same change in force ($P < 0.01$). The increase in slope and shift to longer overall lengths of the active aponeurosis force–length relationship as MTU length increased was likely due to a combination of parallel lengthening of aponeurosis and greater transverse aponeurosis strains. This study provides in vivo evidence that human aponeurosis stiffness is increased from low to moderate forces and that the fascicle strains for a given muscle force are MTU length dependent. Further testing is warranted to determine whether MTU length-dependent stiffness is a fundamental property of the aponeurosis in pennate muscles and evaluate whether this property can enhance muscle performance.

biomechanics | compliance | elastic | fascicle | strain

Animal lower limb muscles typically have two anatomically distinct tendinous structures, which include an extramuscular free tendon and two or three broad aponeurotic sheets. The elastic properties of these tendinous tissues have been shown to be important for maximizing muscle efficiency during locomotion (1, 2), amplifying power output during activities like jumping (3, 4), or attenuating muscle energy absorption during tasks like landing (5). Tendinous tissues store and release energy, respectively, when force from the muscle increases and declines. In many animals, such as wallabies (6), turkeys (7), cats (8), horses (9), and humans (10), the stretch and recoil of the tendinous tissues (which include both tendon and aponeurosis) has been shown to allow lower limb muscle fascicles to operate relatively isometrically during locomotion, which is beneficial for economic force production.

The distinct contributions of the external tendon and aponeurosis to the stretch and recoil of the series elastic element (SEE) during force development have been widely examined, with differences demonstrated between various muscles and contraction conditions (11–15). It is well documented that tendon stiffness increases with force (e.g., refs. 12, 13, 16–18) and that the stiffness remains relatively constant at higher forces (after the compliant toe region) across muscle-tendon unit (MTU) lengths (19–23). However, considerably less is understood about the mechanical behavior of the aponeurosis. The general assumption used in models of muscle-force production (22, 23) is that the aponeurosis behaves as a simple in-series spring. A similar assumption is employed when considering stress–strain relationships of tendinous tissues estimated from muscle fiber/fascicle length changes (7, 10, 24, 25). However, there is a growing body of literature to suggest that the SEE stiffness is dependent on contractile conditions (13, 15, 26–28), as well as suggestions that the aponeurosis cannot be a simple in-series spring (29). The potential variable nature of aponeurosis elastic function is likely to impact our understanding of how this tissue contributes to energy savings and/or power amplification during animal or human locomotion (30), as well as our understanding of the strains experienced by muscles and connective tissues during such contractions and how well we can predict muscle forces using computational models (23).

The force-dependent behavior of the aponeurosis is likely variable and different from the external tendon's behavior because of biaxial loading exhibited in the aponeurosis during contraction. A study by Azizi and Roberts (27) showed that greater transverse strains in the superficial lateral gastrocnemius aponeurosis of turkey muscle increased its longitudinal stiffness during contraction relative to the passive condition. A later investigation on the same muscle found that aponeurosis width increased in direct proportion to muscle fiber shortening at low and intermediate force levels, and that the amount of transverse aponeurosis strain for a given amount of fiber-shortening strain decreased as muscle force increased (28). These findings support the idea that the elastic function of the aponeurosis is not fixed at different force levels and contraction states; however, it is currently unknown if

Significance

Muscle-force production and energy consumption are highly dependent on stiffness of the connecting tendinous tissues (tendon and aponeurosis). Although reduced tendinous tissue stiffness favors greater elastic energy recovery, it permits muscle fiber shortening during fixed-end contractions, which is economically unfavorable for force production. Here, we provide in vivo evidence that the longitudinal central aponeurosis stiffness of human tibialis anterior increases not only with force but also with muscle-tendon unit length. Such a mechanism is likely to be beneficial for different movement scenarios for a range of lower limb muscles. These findings are important for interpreting and modeling muscle-force production and energy consumption during movement and understanding muscle and tendon injury mechanics.

Author contributions: B.J.R., A.G.C., and G.A.L. designed research; B.J.R. performed research; B.J.R. and G.A.L. contributed new reagents/analytic tools; B.J.R. analyzed data; and B.J.R. and G.A.L. wrote the paper.

The authors declare no conflict of interest.

This article is a PNAS Direct Submission. S.S.B. is a guest editor invited by the Editorial Board.

Data deposition: Data from each individual for each of the main outcome measures are available at the following digital object identifier: 10.14264/uql.2017.176.

[1]To whom correspondence should be addressed. Email: brent.raiteri@rub.de.

Published online March 19, 2018.

Table 1. Muscle shear modulus in the superficial TA compartment, dorsiflexion torque, and estimated TA force during isometric contraction at three ankle angles and two muscle forces

Variable	Force condition	Ankle angle, °			*P* value
		80 (DF)	95 (N)	110 (PF)	
Muscle shear modulus, kPa	Low*	55 ± 17	55 ± 15	55 ± 16	0.71
	Moderate	98 ± 21	97 ± 21	99 ± 23	0.41
Dorsiflexion torque, Nm	Low*	6.9 ± 2.8	5.6 ± 2.2	5.3 ± 2.1	
	Moderate	15.9 ± 5.9	12.7 ± 4.7	12.0 ± 4.5	
Predicted TA force, N	Low*	75 ± 23	75 ± 23	76 ± 23	
	Moderate	174 ± 53	176 ± 53	176 ± 54	

Data are presented as mean ± SD. Nm, Newton meter.
*Shear modulus estimates from three participants were excluded in the low force condition because the estimates were not similar across ankle positions.

biaxial loading can modulate the longitudinal aponeurosis stiffness of much larger human muscles.

Another lingering question is whether aponeurosis stiffness is dependent on MTU length, as well as force. For example, Ettema and Huijing (11) and Huijing and Ettema (31) conducted studies on isolated muscle preparations that provide some indirect evidence that strain of the aponeurosis depends on both MTU length and the active state of the muscle. In some elegant follow-up studies, Scott and Loeb (13) showed, in a limited number of cat muscle preparations, that increasing the initial MTU length allowed the aponeurosis length to be comparatively longer when compared at matched isometric force levels. The authors suggested that the variable force versus aponeurosis length relationship was related to variable crimp angles of collagen at different fascicle lengths during contraction, whereby width increases of the aponeurosis at shorter fascicle lengths may increase collagen crimp and subsequently decrease the apparent stiffness of the aponeurosis (13). However, only the direction, and not the magnitude, of aponeurosis width changes was assessed in that study because of limitations with the measurement technique, so it remains unknown if variable transverse aponeurosis strains at different MTU lengths can influence the apparent longitudinal stiffness of the aponeurosis during contraction.

The aim of this study was to determine if the apparent longitudinal stiffness of the human tibialis anterior (TA) central aponeurosis could be modulated by changes in MTU length and force. We hypothesized that aponeurosis longitudinal stiffness would vary with MTU length when compared across the same changes in force levels: specifically, that longer MTU lengths at the time of contraction would increase longitudinal stiffness compared with the same forces at shorter MTU lengths. We further hypothesized that increases in stiffness with increasing MTU length would be driven by increased transverse aponeurosis strains and/or increased initial aponeurosis length at the time of contraction. To achieve these aims, we examined the TA aponeurosis transverse and longitudinal strains, as well as fascicle length changes, at three different MTU lengths in passive muscle and in response to two matched force levels (low and moderate force) during voluntary contraction. The human TA muscle was an ideal model because it has a long internal aponeurotic sheet such that its length and width can be easily quantified (32), and because the TA is the predominant dorsiflexor of the ankle, comprising 48–53% of the entire dorsiflexor physiological cross-sectional area (33). The TA muscle is also superficial, which allows its shear modulus to be estimated during contractions using shear-wave elastography, which was used to provide an index of muscle force (34) and to verify that TA muscle forces were matched across MTU lengths.

Results

Shear Modulus Estimates. Mean TA muscle shear modulus estimates were not significantly different across the MTU lengths tested for both low ($n = 11$) and moderate ($n = 14$) force conditions (Table 1). When the passive muscle shear modulus (Fig. 1) was corrected for fascicle shortening during contraction (35), the mean active forces produced at the short [80° ankle angle, dorsiflexed (DF)] and long [110° ankle angle, plantar-flexed (PF)] MTU lengths were significantly different ($P = 0.05$) in the low force condition. However, in the moderate force condition, mean active forces across the short, moderate [95° ankle angle, neutral (N)], and long MTU lengths were not significantly different ($P = 0.17$; Fig. 2*B*). These results indicate that muscle-specific force levels were similar for each MTU length in the moderate force condition and similar for the two shorter MTU lengths in the low force condition.

Muscle Activity. Surface electromyography (sEMG) revealed that mean normalized TA muscle activity (percentage of maximum voluntary isometric contraction) was significantly higher at the short compared with the moderate and long MTU lengths in the low (10 ± 5%, 7 ± 2%, and 6 ± 3%, respectively; $P \leq 0.02$; $n = 11$) and moderate (24 ± 9%, 15 ± 5%, and 14 ± 4%, respectively; $P < 0.01$; $n = 14$) force conditions, despite similar muscle forces across MTU lengths. There was no significant difference in mean normalized TA muscle activity at the moderate or long MTU lengths for both force conditions ($P = 0.07$ and $P > 0.99$, respectively).

Central Aponeurosis Width and Length Changes. In passive conditions, peak central aponeurosis widths significantly decreased as initial MTU length increased ($P \leq 0.01$, $n = 12$; Fig. 2*A* and Table 2). However, peak central aponeurosis widths were not significantly different across MTU lengths at the low ($P = 0.36$, $n = 9$) or moderate ($P = 0.44$, $n = 12$; Table 2) muscle forces (Fig. 2*A*). A

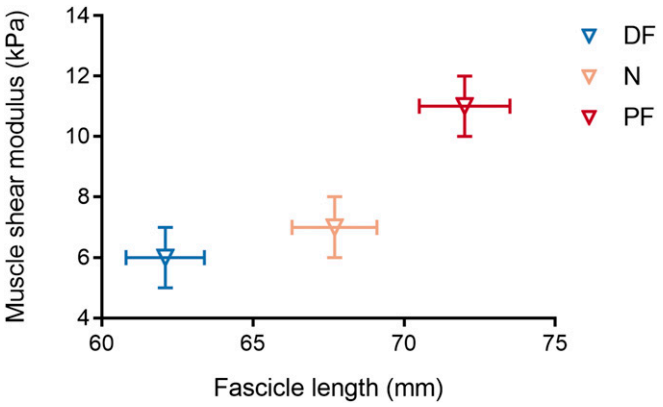

Fig. 1. Mean TA passive muscle shear modulus as a function of mean TA muscle fascicle length in the superficial and deep muscle compartments across the three ankle positions tested (80°, 95°, 110°). Data are presented as mean ± SE.

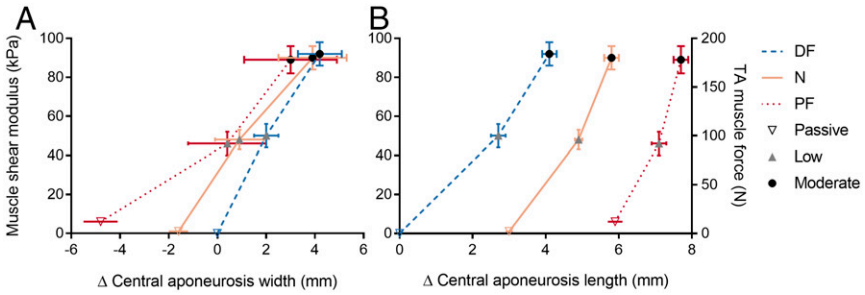

Fig. 2. TA active (low and moderate) and passive muscle shear modulus and estimated TA muscle force as a function of the peak central aponeurosis width (*A*) and central aponeurosis length (*B*) relative to the DF ankle position (shortest MTU length) at rest. The peak central aponeurosis widths and lengths varied across the three ankle positions tested (DF, 80°; N, 95°; PF, 110°) at rest ($n = 12$ and $n = 13$, respectively) and during the low ($n = 9$ and $n = 10$) and moderate ($n = 12$ and $n = 13$) force-matched isometric dorsiflexion contractions. Data are presented as mean ± SE.

comparison of the central aponeurosis width changes when considering the passive to low force change and the low to moderate force change across the ankle positions revealed a significant main effect of MTU length ($P < 0.01$, $n = 9$), but no significant main effect of force ($P = 0.50$). A significant interaction was observed ($P = 0.02$), and Bonferroni post hoc comparisons revealed significantly greater central aponeurosis width changes at the long MTU length compared with the short MTU length ($P < 0.01$; Fig. 2*A*).

Central aponeurosis lengths at rest significantly increased as initial MTU length increased ($P < 0.01$, $n = 13$; Fig. 2*B* and Table 2). However, during contraction, the central aponeurosis lengthened significantly less at longer initial MTU lengths for both the low ($P \leq 0.01$, $n = 10$) and moderate ($P \leq 0.03$, $n = 13$; Table 2) force conditions (Figs. 2*B* and 3*A*). This resulted in a rightward shift and steeper slope of the apparent aponeurosis force-length curve with increasing MTU length (Fig. 2*B*). A comparison of the apparent central aponeurosis stiffnesses when considering the passive to low force change and the low to moderate force change across the ankle positions revealed significant main effects of both force and MTU length ($P < 0.01$, $n = 10$; Fig. 3*B*), but no significant interaction ($P = 0.42$). Central aponeurosis strains were 1.6 ± 0.4%, 1.1 ± 0.3%, and 0.7 ± 0.2% in the low force condition and 2.5 ± 0.5%, 1.7 ± 0.4%, and 1.1 ± 0.3% in the moderate force condition for the short, moderate, and long MTU lengths, respectively. From the passive to low muscle force, the apparent longitudinal central aponeurosis stiffnesses were 30 ± 16 N/mm, 47 ± 26 N/mm, and 68 ± 28 N/mm at the short, moderate, and long MTU lengths, respectively. At the same respective MTU lengths from the low to moderate muscle force, the apparent longitudinal central aponeurosis stiffnesses were 68 ± 15 N/mm, 97 ± 48 N/mm, and 134 ± 69 N/mm. The approximate forces that the apparent stiffness estimates were determined at are presented in Table 1.

Fascicle Length and Pennation Angle Changes. Mean TA fascicle length changes and fascicle rotations decreased as initial MTU length increased during the low ($n = 11$) and moderate ($n = 14$) force-matched isometric dorsiflexion contractions (Fig. 4). A comparison of fascicle length changes in the superficial and deep compartments across the ankle positions at the same muscle force revealed a significant main effect of MTU length only ($P < 0.01$), but no main effect of compartment ($P \geq 0.10$) and no significant interaction ($P \geq 0.95$). The same comparison for pennation angle changes also revealed a significant main effect of MTU length ($P < 0.01$), but no main effect of compartment ($P \geq 0.13$) and no significant interaction ($P \geq 0.45$).

Discussion

The primary aim of this study was to examine if the apparent longitudinal stiffness of the human TA central aponeurosis could be altered by varying initial MTU length during force-matched isometric dorsiflexion contractions. Our results indicate that the aponeurosis is not a simple in-series spring. This result supports previous reports from various animal muscle preparations that have shown the effective longitudinal stiffness of the aponeurosis was greater in the active compared with the passive condition (11, 26, 27, 31). However, our findings also show that the human

Table 2. TA fascicle lengths, pennation angles, and central aponeurosis lengths and widths in the passive and active (moderate force condition) muscle states at three ankle angles

Variable	Muscle state	Ankle angle, °			*P* value
		80 (DF)	95 (N)	110 (PF)	
Superficial compartment fascicle lengths, mm ($n = 14$)	Passive	61.8 ± 7.1	67.4 ± 6.8	71.7 ± 7.1	<0.01
	Active	54.2 ± 6.8	61.9 ± 6.3	68.0 ± 6.5	<0.01
Deep compartment fascicle lengths, mm ($n = 14$)	Passive	66.6 ± 6.8	71.9 ± 6.7	76.1 ± 6.8	<0.01
	Active	59.6 ± 6.1	67.1 ± 6.0	73.1 ± 6.2	<0.01
Superficial compartment pennation angles, ° ($n = 14$)	Passive	10.8 ± 2.0	10.3 ± 1.7	9.5 ± 2.0	<0.01
	Active	12.8 ± 3.0	11.4 ± 2.1	10.2 ± 2.3	<0.01
Deep compartment pennation angles, ° ($n = 14$)	Passive	9.7 ± 2.0	8.6 ± 1.8	7.9 ± 1.8	<0.01
	Active	12.3 ± 2.8	10.6 ± 2.2	9.4 ± 2.0	<0.01
Central aponeurosis lengths, mm ($n = 13$)	Passive	170.0 ± 19.1	173.0 ± 19.0	175.9 ± 19.3	<0.01
	Active	174.1 ± 19.1	175.8 ± 19.0	177.7 ± 19.2	<0.01
Central aponeurosis widths, mm ($n = 12$)	Passive	50.5 ± 8.4	48.9 ± 7.7	45.7 ± 6.8	≤0.01
	Active	54.7 ± 8.7	54.4 ± 8.5	53.5 ± 7.6	0.44

Data are presented as mean ± SD.

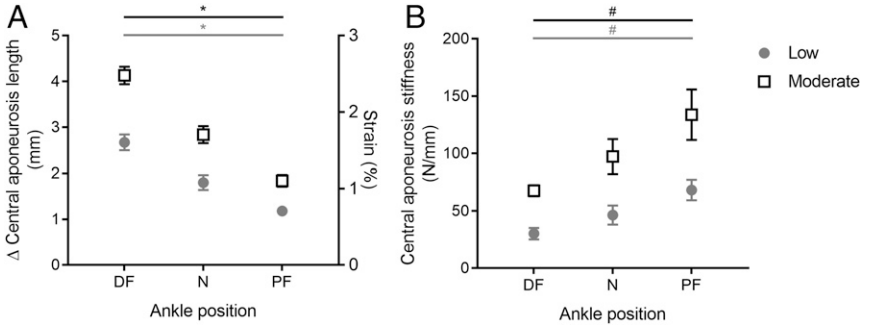

Fig. 3. TA central aponeurosis length changes relative to the passive central aponeurosis length at the same respective MTU length (*A*) and the apparent longitudinal stiffness (*B*) at three ankle positions (DF, 80°; N, 95°; PF, 110°) during low ($n = 10$) and moderate ($n = 13$ and $n = 10$, respectively) force-matched isometric dorsiflexion contractions. Ankle position (MTU length) had a significant main effect on the central aponeurosis length change in both force conditions ($^{*}P \leq 0.03$). Both ankle position and muscle force had significant main effects on the apparent mean TA central aponeurosis stiffness in the longitudinal direction ($^{\#}P < 0.01$), but there was no significant interaction ($P = 0.42$). Data are presented as mean ± SE.

aponeurosis force-length relationship is shifted to longer lengths as MTU length increases and that the initial MTU length seems to influence the slope of its force-length relationship. We found a more compliant central aponeurosis at the shortest MTU length (albeit with greater muscle activity); however, the aponeurosis was shorter at each active force level compared with longer MTU lengths. In contrast, at the longest MTU length, the central aponeurosis was stiffer when the muscle was activated and the aponeurosis was engaged at longer lengths. These findings have implications for our understanding of the potential role of aponeurosis in recycling elastic strain energy during tasks like locomotion.

A key finding of our study was that the apparent active aponeurosis stiffness in the longitudinal direction was greater than the apparent passive aponeurosis stiffness and that the length at which the aponeurosis was engaged upon activation was dependent on the initial MTU length. We postulate that when the muscle was activated, it developed contractile force that acted to stretch the aponeurosis and the free tendon longitudinally, while also increasing the intramuscular pressure: the fluid pressure created by a muscle as it contracts within its fascial compartment (36). It is likely that both intramuscular pressure and fiber bulging, which occurs due to fiber shortening, act to stretch the aponeurosis in width during contraction. This is why at higher muscle forces, where there were greater intramuscular pressures (36) and shorter muscle fibers (Fig. 4), there were also greater aponeurosis widths (Fig. 2*A*). The increase in aponeurosis width during contraction likely caused the increase in the longitudinal stiffness (27, 37), which allowed the aponeurosis to engage at progressively longer lengths as initial MTU length increased and the muscle was subsequently activated.

The initial MTU length likely influenced central aponeurosis length because of the aponeurosis's interaction with the inserting muscle fibers (Fig. 5). As the muscle fascicles were passively lengthened, passive muscle force began to develop and this acted to increase resting central aponeurosis length (Figs. 2*B* and 5*B*). Central aponeurosis width decreased (Figs. 2*A* and 5*A*) because the muscle fibers presumably decreased in width and thickness to remain at a constant volume (38, 39) and their pennation angle also decreased (Table 2), reducing the intramuscular pressure (40, 41). From our data, it is clear that the initial aponeurosis width and length influence its mechanical properties during contraction (Fig. 2); however, we are not able to explain why aponeurosis width changes are greater during contraction at the long MTU length compared with the short MTU length, because intramuscular pressure is likely to be lower at the long MTU length (40, 41) due to the lower pennation angle found at long lengths (Table 2). Similarly, fiber widths are likely to be less at the long MTU length because there was less fiber shortening (Fig. 4), unless active fiber bulging was not symmetrical across MTU lengths. The mechanism for the greater increase in width at a longer length requires further examination.

The stiffness of the aponeurosis in active muscle also varied depending on the MTU length. Based on our data, greater aponeurosis width changes resulted in a smaller aponeurosis length change for the same change in active force (Fig. 2). This finding supports studies on the lateral gastrocnemius aponeurosis of turkeys (27, 28), which showed that higher transverse aponeurosis strains increased aponeurosis stiffness by two- to threefold during active contraction compared with passive muscle stretch (27). The greater transverse strain at longer MTU lengths likely contributed to the increased apparent longitudinal stiffness, demonstrating the importance of biaxial loading in determining the longitudinal stiffness of the aponeurosis.

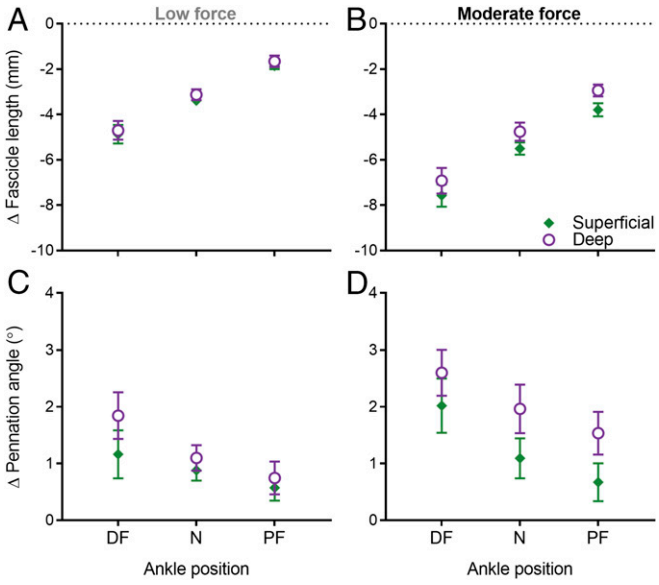

Fig. 4. TA fascicle length (*A* and *B*) and pennation angle (*C* and *D*) changes in the superficial and deep compartments across three ankle positions (DF, 80°; N, 95°; PF, 110°) during low ($n = 11$) and moderate ($n = 14$) force-matched isometric dorsiflexion contractions. The changes are relative to the resting values at the same respective MTU length. MTU length had a significant main effect on the magnitude of fascicle shortening and fascicle rotation ($P < 0.01$), but there was no significant main effect of compartment ($P \geq 0.10$) and no significant interaction ($P \geq 0.45$). Negative values in *A* and *B* indicate shortening. Data are presented as mean ± SE.

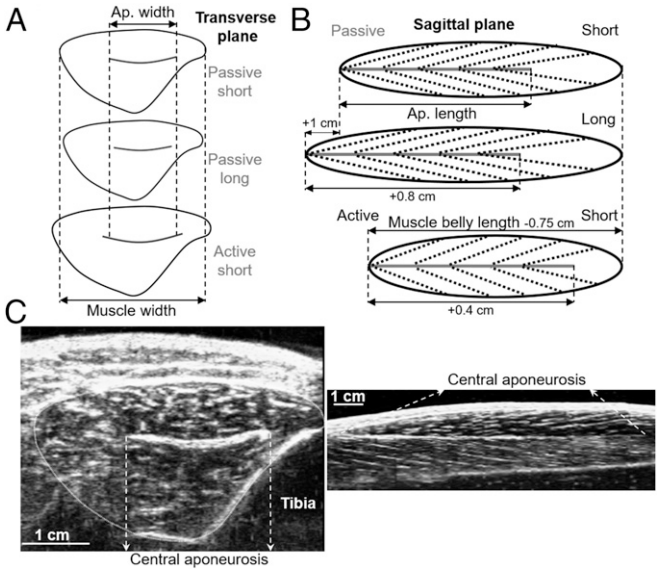

Fig. 5. Passive and active loading of the bipennate TA muscle alters the muscle belly, fascicle, and central aponeurosis strains for a given muscle force. (*A*) Schematic transverse cross-section of the TA midbelly with the central aponeurosis (Ap.) width and muscle width identified. (*B*) Simplified sagittal plane image of the TA muscle belly with the pennate muscle fascicle arrangement with respect to the central Ap. illustrated. (*C*) TA midbelly transverse ultrasound image and a reconstructed parasagittal plane image reslice of the TA from 3DUS imaging at rest. (*A*) As the muscle belly and muscle fibers are passively stretched from short to long lengths, the muscle width and total cross-sectional area decrease slightly. Once the slack of the muscle fibers is taken up, passive force is transmitted to the central aponeurosis, which causes it to decrease in width in the transverse plane (*A*) and to lengthen in the sagittal plane (*B*). Under activation at a fixed short length, muscle width and cross-sectional area increase (*A*) as the muscle fibers shorten and bulge during active force production to remain at a constant volume (*B*), which decreases the muscle belly length. During this period, muscle fiber shortening and bulging, along with increased intramuscular pressure, actively stretch the aponeurosis in width (*A*) and length (*B*), respectively. The white dotted line in *C* highlights the TA cross-sectional area, the white vertical dashed arrows show the most lateral and medial aspects of the central aponeurosis, and the white diagonal dashed arrows show the most distal and proximal aspects of the central aponeurosis.

It is commonly assumed that aponeuroses sit in series with muscle fascicles, and therefore stretch in direct proportion to the force applied (22); however, our data suggest this simplified model is unlikely to be accurate. Our results therefore support theoretical arguments (29) and experimental studies on animal muscle (11, 13, 15, 26, 27, 31) that have disputed the current dogma that aponeurosis is a truly in-series tissue. Our results clearly demonstrate that TA aponeurosis elongation for a given change in muscle force was dependent on the initial passive MTU length. This will have an impact on how energy is stored and returned in the aponeurosis at different MTU lengths, with greater energy storage for a given force at short MTU lengths (where the apparent stiffness was reduced). It was also clear that there was a length-dependent stiffening of the aponeurosis in the presence of muscle activation, which is not accounted for in current models. While further experiments need to be conducted to establish whether these mechanical properties are generalizable to other pennate muscles with long and wide aponeuroses (e.g., human gastrocnemius), a renewed consideration of how aponeurosis stiffness is modeled in musculoskeletal models (e.g., refs. 22, 42, 43) is required. The results of this study also call into question the generalizability of in vivo human aponeurosis stiffness measurements undertaken using ultrasound imaging at a single MTU length or joint angle (14, 44), which do not account for stiffening of the aponeurosis at longer MTU lengths.

The variability in the apparent longitudinal stiffness of the human central aponeurosis directly impacted fascicle shortening magnitudes in each force condition across different MTU lengths. While the small difference in fascicle length changes is likely to have minimal impact on force production according to the length–tension relationship, changes in series compliance may have an impact on fascicle velocity during dynamic contractions (45). Modest reductions in fascicle shortening velocity from a subtle increase in SEE stiffness have been shown to increase twitch torque by as much as 74% and rate of torque development by as much as 154% in the human triceps surae during isometric contractions (46). Therefore, changes in the stiffness of the aponeurosis have the potential to influence force production during contraction considerably.

Our study examined length changes of aponeurosis under isometric conditions; therefore, we can only speculate on the impact that changes in aponeurosis stiffness might have during functional tasks like locomotion. During walking and running, the TA muscle is passively lengthened to long lengths before the foot comes off the ground, upon which the muscle activates to control foot position during leg swing. According to our data, activation at long lengths would stiffen the aponeurosis, allowing the TA muscle fiber length changes to more closely prescribe MTU length changes (47), and hence improve control of foot swing to ensure toe clearance. The TA muscle also absorbs energy when the foot contacts the ground through active lengthening of the MTU. It has been demonstrated that much of this lengthening occurs in the elastic tissues, with the fascicles acting relatively isometrically as the MTU is actively lengthened (47). Engaging the aponeurosis to take up slack at shorter MTU lengths enables energy to be absorbed by the aponeurosis more rapidly compared with passive conditions (47). At this point, such mechanical benefits are only speculative, but further examination of any dynamic benefits of a variable stiffness aponeurosis, based on our findings, is certainly warranted.

In general, length- and force-dependent modulation of aponeurosis stiffness is likely to have the greatest functional impact in pennate muscles with long aponeuroses relative to the muscle fascicles. A recent study on turkey gastrocnemius (28) demonstrated that aponeurosis stiffness certainly increased upon activation of muscle, due primarily to increases in aponeurosis width. However, the length-dependent effect is still yet to be examined in any other pennate muscle. Given that increases in intramuscular pressure and muscle fiber bulging are likely to induce biaxial aponeurosis strains in pennate muscles, it is conceivable that the length-dependent aponeurosis stiffening will also have an impact on storage and return of elastic energy during locomotion in animals, including wallabies, turkeys, humans, and horses (6, 7, 48, 49). In these animals, antigravity muscles (e.g., gastrocnemius) undergo a stretch–shorten cycle, whereby force increases as the MTU is stretched and force decreases as the MTU is shortened. Our results would suggest that the aponeurosis would be able to engage (upon activation) at the short lengths and then progressively stiffen as force and MTU length increase. However, when the muscles are passive, the aponeurosis would provide little resistance to length change, and would therefore enable joint motion to be controlled by the antagonist muscles, unimpeded.

There are a number of minor limitations to the approach taken in our experiment. There is likely to be some effect of creep on the central aponeurosis during the long ∼35-s contractions, which may have resulted in systematic overestimations of central aponeurosis strain relative to the fascicle strains measured during the short ∼2-s contractions. However, this effect is likely to be small and systematic across the ankle positions tested and should not have influenced the main findings of our study. Only moderate force levels were used to ensure that contractions could be sustained during the 3D ultrasound (3DUS) scans (32). However, this was

sufficient to demonstrate the length dependence of the aponeurosis mechanical properties.

Shear modulus was used as an estimate of the passive tension of the TA across the ankle positions (Fig. 1), and although the difference in shear modulus was small, the results showed that the active force produced at the long MTU length was likely to be slightly less than the active force produced at the other MTU lengths in the low force condition (Fig. 2*B*), which may have reduced fascicle shortening and central aponeurosis lengthening at the long MTU length. However, the TA passive forces during the contractions in the moderate force condition were minimal across the MTU lengths, so our results of a variable stiffness of the aponeurosis across MTU lengths must still be valid for this force and for the short and moderate MTU lengths in the low force condition. Our shear modulus values were estimated along the longitudinal direction of superficial muscle fibers with a small pennation angle that did not vary, on average, by more than 3° (Table 2), so we believe that tissue anisotropy was unlikely to have influenced our measurements across MTU lengths (50).

Finally, our study used human TA muscle-tendon moment arm values from the literature (51) rather than determining these for each individual. TA moment arms are likely to vary between individuals, and TA moment arm depends on muscle force (51), both of which likely influenced our estimates of TA muscle force. For this reason, we measured the muscle shear modulus, which is used as an index of muscle force (34), to help verify that our forces were at least consistent across joint positions. While we had to exclude data from three participants because their TA shear modulus values varied by more than 15% across the MTU lengths, the trends of length change of the aponeurosis from the low force to moderate force condition were consistent across MTU lengths and individuals. Therefore, we are confident that our force-matching protocol was sufficient to demonstrate the principle of variable human aponeurosis mechanical properties in the longitudinal direction as a function of MTU length.

Methods

Participants. Fourteen healthy participants (eight males) with a mean ± SD for age of 26 ± 3 y, body mass of 74 ± 11 kg, and height of 175 ± 7 cm, with no preexisting neuromuscular disorders and no recent history (<12 mo) of lower limb surgery or injury, participated in the study. Subjects were not participating in regular strenuous exercise during the testing week and provided written informed consent before participation. The study protocol was approved (HMS14/0704) and endorsed by the University of Queensland Human Research Ethics Committee and conducted in accordance with the Declaration of Helsinki.

Experimental Setup and Protocol. Participants were side-lying on their right hip on a cushioned bench (Fig. 6). Their left hip was in a N position, their left knee was fully extended, and their left foot was positioned flush against the footplate attachment of an isokinetic dynamometer (Biodex System 3 Pro; Biodex Medical Systems), with the ankle at 90° (sole of foot perpendicular to the shank). The ankle joint center (approximated from the lateral malleolus) was visually aligned with the axis of rotation of the dynamometer at this joint angle. Dorsiflexion torque was measured from the dynamometer and low-pass-filtered at 25 Hz, before being analog-to-digitally converted at 2 kHz using a 16-bit Micro3 1401 (Cambridge Electronic Design).

Before testing, participants performed five voluntary submaximal (1-s hold, 1-s rest, to ∼80% of maximum) isometric dorsiflexion contractions at an ankle angle of 80° (10° dorsiflexion) to precondition the MTU (52). Following this, at least two maximal (3-s hold) isometric dorsiflexion contractions were performed in a randomized order at ankle angles of 80°, 95° (5° plantar flexion), and 110° (20° plantar flexion), which will be referred to as the DF, N, and PF ankle positions (short, moderate, and long MTU lengths, respectively) from this point forward.

Participants performed at least three ∼2-s isometric dorsiflexion contractions at each of the DF, N, and PF ankle positions (to alter the initial MTU length) at two muscle forces. The muscle forces corresponded to 15% (low force condition) and 35% (moderate force condition) of the maximum dorsiflexion force produced in the N ankle position (Fig. 6). Two-dimensional ultrasound imaging and sEMG recordings were performed during the contractions, and at least 10 s was provided between contractions, with the low and moderate force-matched contractions being alternated at the same ankle position.

Two passive ankle dorsiflexion movements were then imposed at a constant velocity of 1° per second from 25° of plantar flexion to 15° of dorsiflexion to estimate passive force reductions due to fascicle shortening during the fixed-end contractions. A passive rotation was repeated if there was a visible increase in TA sEMG. The protocol described above constituted the

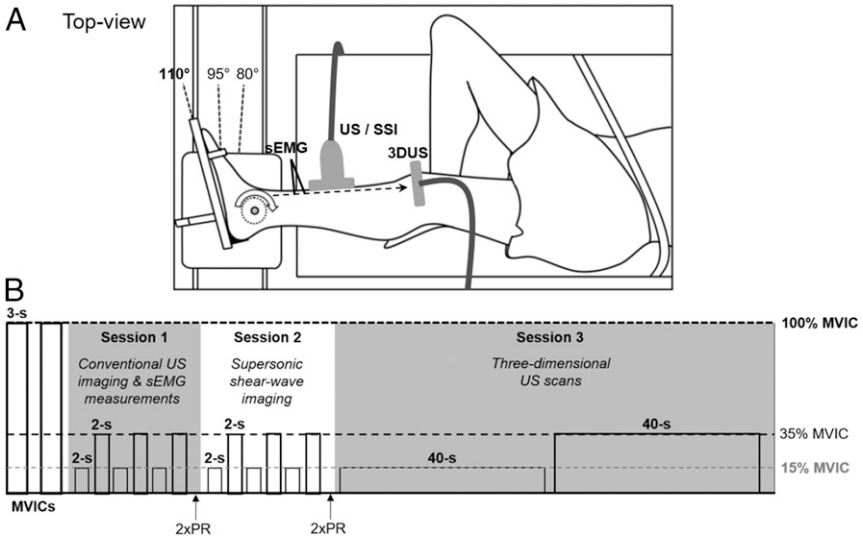

Fig. 6. Experimental setup and protocol performed at the N (95°) ankle position. (*A*) Location of the veterinary ultrasound (US) transducer was identical to the SSI transducer (shown) and the computer screen that provided torque feedback was located 1 m in front of the participant's face at eye level. The two solid lines indicate where the sEMG electrodes were located, and the dashed arrow indicates the direction of the 3DUS imaging. (*B*, *Left*) Rectangular bars indicate when an isometric dorsiflexion contraction was performed, and the numbers above the bars indicate the contraction duration in seconds. (*B*, *Right*) Scale indicates the contraction intensity. The maximum voluntary isometric contractions (MVICs) were immediately repeated at the DF (80°) and PF (110°) ankle positions with at least 2 min of rest provided between contractions. Similarly, contractions within sessions 1–3 were immediately repeated at the DF and PF ankle positions, with the contractions being performed at equivalent low and moderate muscle forces.

first part of the experiment, and this protocol was repeated with supersonic shear-wave imaging (SSI) to make up the second part of the experiment.

For the third part of the experiment, participants performed at least one ~40-s isometric dorsiflexion contraction at the same two muscle forces and ankle positions described above (Fig. 6). This resulted in a minimum of six sustained contractions, which were separated by at least 60 s of rest. Free-hand 3DUS scans were performed at rest and during the sustained contractions to assess central aponeurosis lengths and widths. The order in which the ankle positions were tested was randomized for each of the three parts that constituted the experiment.

Muscle-Force Predictions. The two submaximal TA muscle forces that were matched across the ankle positions were defined as 15% (low) and 35% (moderate) of the maximum torque attained in the N ankle position (Fig. 6 and Table 3), divided by a resting TA moment arm estimate of 0.033 m (51):

$$F_{low} = DF_{mvc} * 0.15/MA_n, \quad [1]$$

$$F_{mod} = DF_{mvc} * 0.35/MA_n, \quad [2]$$

where F_{low} and F_{mod} are the required low and moderate forces, respectively, required during testing in the N ankle position; DF_{mvc} is the maximum active dorsiflexion torque produced in the N ankle position; and MA_n corresponds to the estimated TA resting moment arm in the N ankle position. The low and moderate dorsiflexion torques required to match the low and moderate forces in the DF and PF ankle positions were then calculated by multiplying the respective forces (calculated in Eqs. **1** and **2**) by the estimated resting TA moment arms [0.0413 m and 0.0313 m (51), respectively]. The required dorsiflexion torques to match the required forces across ankle positions for a theoretical participant who produces a DF_{mvc} of 50 Newton meter (Nm) in the N ankle position is provided for reference in Table 3.

At each ankle position, passive ankle torque, synergistic torque contributions, and muscle co-contraction were neglected (35, 53), and participants received on-line visual feedback on their dorsiflexion torque relative to time via a monitor positioned in front of them while they tried to match one of the six dorsiflexion torques. To ensure that participants produced similar forces at each ankle position, subjects were instructed to keep their dorsiflexion torque within two horizontal cursors that were positioned 2.5% above and below the predefined dorsiflexion torque. If the dorsiflexion torque fell outside either of these cursors for more than 1 s, the trial was excluded and repeated.

Two-Dimensional Ultrasound Imaging. Fascicle length and pennation angle changes of TA during contraction were recorded using a flat, linear, 96-element transducer (LV7.5/60/96; Telemed) attached to a PC-based ultrasound system (Echoblaster 128, UAB; Telemed). The transducer was secured over the approximate midbelly of the TA using an adhesive bandage and was used to image muscle fascicles in the superficial and deep compartments, as well as between superficial, central, and deep aponeuroses, in an image plane that had the clearest image of continuous muscle fascicles and aponeuroses both at rest and during contraction. Ultrasound images were captured using Echowave II software (Telemed) at a frequency of 6 MHz, with a field of view of 60 × 50 mm (width × depth) and a frame rate of 80 Hz, and were synchronized with collection of all analog data (35). Fascicle lengths and pennation angles of TA were measured in each image using previously described tracking software and procedures (54, 55).

Table 3. Estimated dorsiflexion torques required for constant low and moderate TA forces across three ankle positions for a theoretical participant who produces a maximum voluntary dorsiflexion torque of 50 Nm at a 95° ankle angle

AA, °	TA MA, cm	Force condition	TA force, N	Torque, Nm
80 (DF)	4.13	Low	227	9.4
		Moderate	530	21.9
95 (N)	3.30	Low	227	7.5
		Moderate	530	17.5
110 (PF)	3.13	Low	227	7.1
		Moderate	530	16.6

Resting TA moment arm (MA) numbers were obtained from Maganaris et al. (51). AA, ankle angle.

SSI. An SSI ultrasound scanner (Aixplorer, v. 9.0; Supersonic Imagine) with a linear transducer array (4–15 MHz, SL15-4) and musculoskeletal preset was used to estimate the TA muscle shear modulus in the superficial compartment at 1.3–1.9 Hz during the contractions (optimization = penetration, persistence = off, smoothing = 9). The ultrasound transducer was positioned over the TA muscle using the same protocol as for 2D imaging. The transducer was then maintained in this position and orientation by the investigator with very light pressure so that the transducer was only in contact with the echogenic gel applied over the skin. If the transducer orientation changed at rest or during contraction, then this was apparent from the B-mode ultrasound image and the trial was repeated. After the images were captured, color maps of the shear modulus were exported in "mp4" format, sequenced into "jpeg" images, and analyzed as described previously by Raiteri et al. (53). This process involved using the recorded color scale to convert each pixel of the color map into a value of shear modulus (56).

sEMG. sEMG of TA was recorded using a bipolar configuration with two electrodes (8-mm recording diameter, Ag/AgCl; Covidien) spaced 2 cm apart (center-to-center). The electrode position was immediately distal to the ultrasound transducer. Electrodes were secured to the skin after the skin was shaved, abraded, and cleaned with alcohol. A reference electrode was placed on the left ankle over the medial malleolus. The sEMG signals were amplified 1,000-fold (Neurolog System; Digitimer) and filtered with a band-pass analog filter between 10 and 500 Hz, before being sampled at 2 kHz using a 16-bit Micro3 1401 and Spike2 data collection system (Cambridge Electronics Design).

3DUS Imaging. The 3D TA muscle and central aponeurosis deformations were imaged using 3DUS. The 3DUS scan involved tracking of the ultrasound transducer position and orientation (Motive; Natural Point) in combination with synchronous B-mode ultrasound imaging (SonixTouch; Ultrasonix) using Stradwin software (v5.1; Cambridge University), as described in detail by Raiteri et al. (32). The system was temporally and spatially calibrated in Stradwin (57) before testing, as has been described in detail elsewhere (58).

Transverse images of the soft tissues within the left shank were recorded using a linear transducer (L14-5W/60 Linear; Ultrasonix) with a central frequency of 10 MHz and a field of view of 60 × 55 mm (width × depth). The average distance between frames was ~1 mm, and the frame rate was ~10–15 Hz. A 2-cm-thick echogenic ultrasound gel pad (Aquaflex; Parker Laboratories), which conformed to the shape of the shank when light constant pressure was applied, was positioned between the transducer and the skin to ensure that the transverse images contained visible TA borders for the majority of the scan. Each scan lasted ~35 s.

Data Analysis. To determine TA muscle activity from sEMG measurements, a 100-ms sliding window was moved 1 ms at a time to calculate the root mean square (rms) amplitudes for each contraction when conventional ultrasound imaging was performed. Background sEMG activity was calculated as the mean rms amplitude over ~0.5 s when participants were instructed to relax. This resting value was subtracted from the rms amplitude calculated over 1 s during each contraction when there was a constant dorsiflexion torque. The rms amplitudes for each trial were then normalized to the peak rms amplitude achieved during the maximal dorsiflexion contraction at the same ankle position to provide normalized muscle activities.

Changes in muscle fascicle length and pennation angle during contraction were calculated by subtracting the mean fascicle length and pennation angle in the resting state (mean values over ~0.5 s when participants were instructed to relax) from the mean fascicle length and pennation angle calculated over 1 s during each contraction when there was a constant dorsiflexion torque. Mean changes in fascicle lengths and pennation angles were then averaged across trials.

Consecutive muscle shear modulus values within 5 kPa of each other at the predefined dorsiflexion torques were averaged for each trial. To satisfy the criterion for a constant muscle force across joint positions, the mean shear modulus of at least one trial in one ankle position could not differ by more than 15% from at least one trial in the other two ankle positions. If this criterion was not met, then the shear modulus data and all other data associated with that force-matched condition and participant (e.g., muscle activities, fascicle lengths, central aponeurosis widths/lengths) were excluded from analysis.

TA central aponeurosis length was calculated as the straight-line distance between the most distal and proximal landmark locations in 3D space. The TA force along its longitudinal axis was estimated for each participant by multiplying the target dorsiflexor force by the TA's relative physiological cross-sectional area as a percentage of the dorsiflexor's physiological cross-sectional area, which is ~50% (33). This TA force (which accounted for the

torque contributions of all synergist muscles) was then divided by the central aponeurosis length change (relative to the resting aponeurosis length for the same respective MTU length) during contraction to calculate the apparent longitudinal central aponeurosis stiffness from the passive to low force condition. The apparent aponeurosis stiffness from the low to moderate force condition was calculated as the change in TA force from the low to moderate force divided by the central aponeurosis length change from the low to moderate force at the same respective MTU length.

The central aponeurosis was manually outlined along its width medially to laterally in the transverse images using landmarks that were spaced sequentially at 10-mm intervals along the length of the central aponeurosis. The 3D positions of the central aponeurosis landmarks within the laboratory reference frame were later exported for postprocessing in MATLAB (R2014b; MathWorks), and a weighted principal component analysis was performed to determine the longitudinal axis of the central aponeurosis (32).

For each analysis, data from three participants were excluded in the low force condition because muscle forces were not matched across ankle positions, as estimated by the muscle shear modulus. Consequently, muscle activity, fascicle length, and pennation angle data from 11, and not 14, participants are included for the low force condition. Central aponeurosis reconstructions from two participants were also excluded from analysis for both force conditions because of difficulties in visualizing the central aponeurosis or unreliable reconstructions because of high curvature and/or irregular shape of the aponeurosis. This resulted in central aponeurosis width data from nine and 12 participants for the low and moderate force-matched conditions, respectively. For central aponeurosis length analysis, one additional participant was excluded because the quality of that individual's 3DUS scans was insufficient to determine the aponeurosis end points. This resulted in central aponeurosis length measurements from 10 and 13 participants for the low and moderate force conditions, respectively, and central aponeurosis stiffness measurements from 10 participants.

Statistics. Statistical analysis was performed using commercially available software (Prism 6; GraphPad), and data were assessed for normality using Shapiro–Wilk normality tests. In cases where normality was violated, a natural logarithmic transform was applied and analyzed to determine if it passed normality. If the transformed data were not normally distributed or if any of the nontransformed values were negative, a nonparametric test equivalent to the parametric comparison was implemented. One-way repeated-measures ANOVAs or Friedman tests were used to assess differences in muscle shear modulus values, normalized muscle activities, and central aponeurosis length changes relative to rest across all ankle positions at the low or moderate muscle force. These same tests were also used to assess differences across the ankle positions in passive central aponeurosis lengths and relative length changes at each active force level, as well as peak central aponeurosis widths in each force condition. In cases where sphericity was violated for the ANOVA, a Greenhouse–Geisser correction was performed. If a main effect was observed, Bonferroni or Dunn's (for nonnormally distributed data) post hoc tests were performed to determine the ankle positions that were significantly different from each other.

Differences in fascicle length or pennation angle changes between the TA muscle compartments across the ankle positions (MTU lengths) at each muscle force were compared using two-way repeated-measures ANOVAs (ankle position × muscle compartment; note that the muscle compartment was treated independently). Two-way repeated-measures ANOVAs were also used to compare central aponeurosis width changes and apparent central aponeurosis stiffnesses when considering the passive to low force changes and low to moderate force changes across the ankle positions (ankle position × force condition; note that the force condition was treated independently). If a significant interaction was observed, Bonferroni post hoc tests were performed to determine the ankle positions that were significantly different from each other across both force conditions. All data are presented as mean ± SD in the text and mean ± SE in the figures. The level of significance was set at $P \leq 0.05$.

ACKNOWLEDGMENTS. We thank E. Jenkins for assistance during experiments. We also acknowledge the insightful comments and suggestions from the anonymous reviewers. Infrastructure support came from The University of Queensland, and financial support came from an Australian Postgraduate Award (to B.J.R.).

1. Alexander RM, Maloiy GMO, Ker RF, Jayes AS, Warui CN (1982) The role of tendon elasticity in the locomotion of the camel (Camelus dromedarius). *J Zool* 198:293–313.
2. Lichtwark GA, Wilson AM (2007) Is Achilles tendon compliance optimised for maximum muscle efficiency during locomotion? *J Biomech* 40:1768–1775.
3. Aerts P (1998) Vertical jumping in Galago senegalensis: The quest for an obligate mechanical power amplifier. *Proc Biol Sci* 353:1607–1620.
4. Roberts TJ, Marsh RL (2003) Probing the limits to muscle-powered accelerations: Lessons from jumping bullfrogs. *J Exp Biol* 206:2567–2580.
5. Roberts TJ, Konow N (2013) How tendons buffer energy dissipation by muscle. *Exerc Sport Sci Rev* 41:186–193.
6. Biewener AA, Konieczynski DD, Baudinette RV (1998) In vivo muscle force-length behavior during steady-speed hopping in tammar wallabies. *J Exp Biol* 201: 1681–1694.
7. Roberts TJ, Marsh RL, Weyand PG, Taylor CR (1997) Muscular force in running turkeys: The economy of minimizing work. *Science* 275:1113–1115.
8. Maas H, Gregor RJ, Hodson-Tole EF, Farrell BJ, Prilutsky BI (2009) Distinct muscle fascicle length changes in feline medial gastrocnemius and soleus muscles during slope walking. *J Appl Physiol (1985)* 106:1169–1180.
9. Butcher MT, et al. (2009) Contractile behavior of the forelimb digital flexors during steady-state locomotion in horses (Equus caballus): An initial test of muscle architectural hypotheses about in vivo function. *Comp Biochem Physiol A Mol Integr Physiol* 152:100–114.
10. Lichtwark GA, Wilson AM (2006) Interactions between the human gastrocnemius muscle and the Achilles tendon during incline, level and decline locomotion. *J Exp Biol* 209:4379–4388.
11. Ettema GJ, Huijing PA (1989) Properties of the tendinous structures and series elastic component of EDL muscle-tendon complex of the rat. *J Biomech* 22:1209–1215.
12. Lieber RL, Leonard ME, Brown CG, Trestik CL (1991) Frog semitendinosis tendon load-strain and stress-strain properties during passive loading. *Am J Physiol* 261:C86–C92.
13. Scott SH, Loeb GE (1995) Mechanical properties of aponeurosis and tendon of the cat soleus muscle during whole-muscle isometric contractions. *J Morphol* 224:73–86.
14. Maganaris CN, Paul JP (2000) Load-elongation characteristics of in vivo human tendon and aponeurosis. *J Exp Biol* 203:751–756.
15. Lieber RL, Leonard ME, Brown-Maupin CG (2000) Effects of muscle contraction on the load-strain properties of frog aponeurosis and tendon. *Cells Tissues Organs* 166: 48–54.
16. Proske U, Morgan DL (1984) Stiffness of cat soleus muscle and tendon during activation of part of muscle. *J Neurophysiol* 52:459–468.
17. Rack PM, Westbury DR (1984) Elastic properties of the cat soleus tendon and their functional importance. *J Physiol* 347:479–495.
18. Ker RF (1981) Dynamic tensile properties of the plantaris tendon of sheep (Ovis aries). *J Exp Biol* 93:283–302.
19. Rack PM, Westbury DR (1974) The short range stiffness of active mammalian muscle and its effect on mechanical properties. *J Physiol* 240:331–350.
20. Walmsley B, Proske U (1981) Comparison of stiffness of soleus and medial gastrocnemius muscles in cats. *J Neurophysiol* 46:250–259.
21. Morgan DL (1977) Separation of active and passive components of short-range stiffness of muscle. *Am J Physiol* 232:C45–C49.
22. Zajac FE (1989) Muscle and tendon: Properties, models, scaling, and application to biomechanics and motor control. *Crit Rev Biomed Eng* 17:359–411.
23. Sandercock TG, Heckman CJ (1997) Force from cat soleus muscle during imposed locomotor-like movements: Experimental data versus Hill-type model predictions. *J Neurophysiol* 77:1538–1552.
24. van Ingen Schenau GJ, Bobbert MF, de Haan A (1997) Mechanics and energetics of the stretch-shortening cycle: A stimulating discussion. *J Appl Biomech* 13:484–496.
25. Griffiths RI (1991) Shortening of muscle fibres during stretch of the active cat medial gastrocnemius muscle: The role of tendon compliance. *J Physiol* 436:219–236.
26. Zuurbier CJ, Everard AJ, van der Wees P, Huijing PA (1994) Length-force characteristics of the aponeurosis in the passive and active muscle condition and in the isolated condition. *J Biomech* 27:445–453.
27. Azizi E, Roberts TJ (2009) Biaxial strain and variable stiffness in aponeuroses. *J Physiol* 587:4309–4318.
28. Arellano CJ, Gidmark NJ, Konow N, Azizi E, Roberts TJ (2016) Determinants of aponeurosis shape change during muscle contraction. *J Biomech* 49:1812–1817.
29. Epstein M, Wong M, Herzog W (2006) Should tendon and aponeurosis be considered in series? *J Biomech* 39:2020–2025.
30. Roberts TJ, Azizi E (2011) Flexible mechanisms: The diverse roles of biological springs in vertebrate movement. *J Exp Biol* 214:353–361.
31. Huijing PA, Ettema GJ (1988–1989) Length-force characteristics of aponeurosis in passive muscle and during isometric and slow dynamic contractions of rat gastrocnemius muscle. *Acta Morphol Neerl Scand* 26:51–62.
32. Raiteri BJ, Cresswell AG, Lichtwark GA (2016) Three-dimensional geometrical changes of the human tibialis anterior muscle and its central aponeurosis measured with three-dimensional ultrasound during isometric contractions. *PeerJ* 4:e2260.
33. Brand RA, Pedersen DR, Friederich JA (1986) The sensitivity of muscle force predictions to changes in physiologic cross-sectional area. *J Biomech* 19:589–596.
34. Hug F, Tucker K, Gennisson J-L, Tanter M, Nordez A (2015) Elastography for muscle biomechanics: Toward the estimation of individual muscle force. *Exerc Sport Sci Rev* 43:125–133.
35. Raiteri BJ, Cresswell AG, Lichtwark GA (2015) Ultrasound reveals negligible cocontraction during isometric plantar flexion and dorsiflexion despite the presence of antagonist electromyographic activity. *J Appl Physiol (1985)* 118:1193–1199.
36. Aratow M, et al. (1993) Intramuscular pressure and electromyography as indexes of force during isokinetic exercise. *J Appl Physiol (1985)* 74:2634–2640.

37. Lanir Y, Fung YC (1974) Two-dimensional mechanical properties of rabbit skin. II. Experimental results. *J Biomech* 7:171–182.
38. Elliott GF, Lowy J, Worthington CR (1963) An X-ray and light-diffraction study of the filament lattice of striated muscle in the living state and in rigor. *J Mol Biol* 6:295–305.
39. Huxley HE (1953) X-ray analysis and the problem of muscle. *Proc R Soc Lond B Biol Sci* 141:59–62.
40. Ateş F, et al. (2018) Intramuscular pressure of tibialis anterior reflects ankle torque but does not follow joint angle-torque relationship. *Front Physiol* 9:22.
41. Styf J, et al. (1995) Intramuscular pressure and torque during isometric, concentric and eccentric muscular activity. *Scand J Med Sci Sports* 5:291–296.
42. Delp SL, et al. (2007) OpenSim: Open-source software to create and analyze dynamic simulations of movement. *IEEE Trans Biomed Eng* 54:1940–1950.
43. Anderson FC, Pandy MG (2001) Dynamic optimization of human walking. *J Biomech Eng* 123:381–390.
44. Magnusson SP, Aagaard P, Dyhre-Poulsen P, Kjaer M (2001) Load-displacement properties of the human triceps surae aponeurosis in vivo. *J Physiol* 531:277–288.
45. Hill AV (1949) The abrupt transition from rest to activity in muscle. *Proc R Soc Lond B Biol Sci* 136:399–420.
46. Mayfield DL, Cresswell AG, Lichtwark GA (2016) Effects of series elastic compliance on muscle force summation and the rate of force rise. *J Exp Biol* 219:3261–3270.
47. Chleboun GS, Busic AB, Graham KK, Stuckey HA (2007) Fascicle length change of the human tibialis anterior and vastus lateralis during walking. *J Orthop Sports Phys Ther* 37:372–379.
48. Lichtwark GA, Bougoulias K, Wilson AM (2007) Muscle fascicle and series elastic element length changes along the length of the human gastrocnemius during walking and running. *J Biomech* 40:157–164.
49. Biewener AA (1998) Muscle-tendon stresses and elastic energy storage during locomotion in the horse. *Comp Biochem Physiol B Biochem Mol Biol* 120:73–87.
50. Miyamoto N, Hirata K, Kanehisa H, Yoshitake Y (2015) Validity of measurement of shear modulus by ultrasound shear wave elastography in human pennate muscle. *PLoS One* 10:e0124311.
51. Maganaris CN, Baltzopoulos V, Sargeant AJ (1999) Changes in the tibialis anterior tendon moment arm from rest to maximum isometric dorsiflexion: In vivo observations in man. *Clin Biomech (Bristol, Avon)* 14:661–666.
52. Maganaris CN, Baltzopoulos V, Sargeant AJ (2002) Repeated contractions alter the geometry of human skeletal muscle. *J Appl Physiol (1985)* 93:2089–2094.
53. Raiteri BJ, Hug F, Cresswell AG, Lichtwark GA (2016) Quantification of muscle cocontraction using supersonic shear wave imaging. *J Biomech* 49:493–495.
54. Gillett JG, Barrett RS, Lichtwark GA (2013) Reliability and accuracy of an automated tracking algorithm to measure controlled passive and active muscle fascicle length changes from ultrasound. *Comput Methods Biomech Biomed Engin* 16:678–687.
55. Farris DJ, Lichtwark GA (2016) UltraTrack: Software for semi-automated tracking of muscle fascicles in sequences of B-mode ultrasound images. *Comput Methods Programs Biomed* 128:111–118.
56. Ateş F, et al. (2015) Muscle shear elastic modulus is linearly related to muscle torque over the entire range of isometric contraction intensity. *J Electromyogr Kinesiol* 25: 703–708.
57. Prager RW, Rohling RN, Gee AH, Berman L (1998) Rapid calibration for 3-D freehand ultrasound. *Ultrasound Med Biol* 24:855–869.
58. Barber L, Barrett R, Lichtwark G (2009) Validation of a freehand 3D ultrasound system for morphological measures of the medial gastrocnemius muscle. *J Biomech* 42: 1313–1319.